RSC Advances

PAPER

View Article Online
View Journal | View Issue

Cite this: *RSC Adv.*, 2019, **9**, 24451

Optimisation of compatibility for improving elongation at break of chitosan/starch films

Kai-qiang Sun,[ab] Fang-yi Li, *[ab] Jian-yong Li,*[ab] Jian-feng Li,[ab] Chuan-wei Zhang,[ab] Shuai Chen,[ab] Xu Sun[ab] and Jin-feng Cui[ab]

When chitosan/starch films were used as agricultural mulch films, the problem of rupture often occurred. In order to improve the elongation at break, chitosan/starch blend films were prepared by casting with different formulations (different ratios of chitosan to starch, different plasticizing components and different plasticizer ratios) in this research. The elongation at break of the film reached up to 104.1% when chitosan was plasticized with 10% glycerol and 0.94% ethylene glycol alone and then mixed according to a 1 : 0.6 chitosan–starch ratio. The fact that plasticizing starch, plasticizing chitosan or co-plasticizing starch and chitosan made a big difference to the mechanical properties of the films was discovered for the first time. The films with different plasticizing components were characterized by their mechanical properties, crystal structures and surface morphologies. Mechanical properties of the films were related to their crystallinity. The higher the crystallinity, the higher the elongation at break. Plasticizing starch alone facilitated the formation of hydrogen bonds and massive structures. Plasticizing chitosan alone was beneficial to the formation of network structures of the films and exhibited anti-plasticization at low plasticizer concentration.

Received 30th May 2019
Accepted 19th July 2019

DOI: 10.1039/c9ra04053f

rsc.li/rsc-advances

1. Introduction

Plastic waste poses a serious threat to the environment and human health.[1] Finding fully degradable natural polymer materials to replace plastics is currently a hot topic.[2] Agricultural mulch films are widely used in crop protection, as they can retain heat and moisture, improve the utilisation of solar energy, and protect plant roots. Most of these films remain in the form of debris in the soil, thereby causing heavy metal contamination of the soil and impeding soil permeability.[3] Therefore, the development and utilization of degradable films has become a trend. Among the existing degradable materials, natural biopolymers (*i.e.* starch) have huge advantages compared to synthetic biodegradable polymers as they are renewable, widely available, degradable and are fully compostable and free of toxic residues.[4]

However, starch films are limited in application due to their poor mechanical properties and poor water resistance.[5,6] To overcome these shortcomings, researchers have studied a number of methods, including: (1) physical modification: ultrasonic treatment of starch films to increase its elongation at break.[7] (2) Chemical modification: plastic modification,[8,9] cross-linking modification,[10,11] *etc.* to improve mechanical properties; (3) blending modification: mixing sugar palm nanocrystalline cellulose[12–14] to improve the waterproofness and degradability,[15,16] adding chitosan[17–19] to improve the mechanical properties and waterproofness. Among all the improvements, chitosan has good antibacterial properties[20] and biocompatibility.[21,22] The prepared chitosan/starch films as agricultural mulch films can serve as fertilisers to nourish crops after full degradation and keep seeds away from harmful bacteria. Therefore, it is a good choice to replace agricultural plastic films. However, when the chitosan/starch films are used as an agricultural mulch film, the problem of film rupture often occurred. Hence, the elongation at break of such films must be increased. The mechanical properties of chitosan and starch at different ratios and with concentration gradients of 0.5 were compared in the study by Xu *et al.* The results showed that the tensile strength and elongation of the films increase first and then decrease as starch content increases. The maximum elongation at break of the film can reach 60%.[23] Therefore, by changing the ratio of chitosan to starch, the elongation at break of the films can be increased. However, the exact ratio of chitosan to starch at the highest elongation at break has not been explored. In addition, it has been widely proved that plasticizing modification can improve the mechanical properties of the films.[9,10,24,25] The results of Natta laohakunjit *et al.* showed that glycerol, sorbitol and ethylene glycol had different effects on the mechanical properties of starch films when used as plasticizers.[9] It was found that glycerol molecules were probably bound to the acetamide group of chitosan by H-bonds, which

[a]*Key Laboratory of High Efficiency and Clean Mechanical Manufacture, Ministry of Education, School of Mechanical Engineering, Shandong University, Jinan 250061, China. E-mail: lifangyi@sdu.edu.cn*

[b]*National Demonstration Center for Experimental Mechanical Engineering Education, Shandong University, Jinan 250061, China*

prevents the acetamide groups from forming interchain H-bonds with other chitosan molecules, and leads to breakdown of the intermolecular connectivity between the polysaccharide chains, seen in Attila Domjan's research. It also showed that no stable connection was found between the PEG 400 molecules and the polysaccharide chains, but the H-bonds formed by the amide groups were reduced.[26] The above studies found that glycerin and polyethylene glycol were both good plasticizer for chitosan and starch. So these two reagents were chosen as plasticizers in this research. H. H. Liu *et al.* used glycerine as a plasticizer to improve the mechanical properties of chitosan/starch films. The research showed that adding 5% and higher concentrations of glycerine leads to a decrease in tensile strength and an increase in elongation at break.[24] It was found that different concentrations of glycerol changed the elongation at break of the chitosan/starch films by affecting the formation of hydrogen bonds between chitosan and starch in Cholwasa Bangyekan's research.[25] The results of Natta lahakunjit *et al.* showed that different plasticizers changed the solid crystallinity of the chitosan/starch films, which in turn affects the properties of the films.[27] Tuhin *et al.* used glycerine and mustard oil as plasticizer. The research showed that the elongation at break of the films exerts different effects depending on the proportion of plasticizer.[28] The above studies showed that different concentrations of plasticizers had a greater impact on the elongation at break of the chitosan/starch films.

In summary, increasing the elongation at break of films requires changing the ratio of chitosan to starch and the ratio of plasticizers. In addition to the two methods, the current study also showed that plasticisation of different components also affected the mechanical properties of films. In this study, the elongation at break of films under different ratios of chitosan and starch was compared by controlled variable method. The ratio of glycerol to ethylene glycol at the time of maximum elongation at break of the films was obtained by uniform experiment and calculation analysis. Finally, the optimal compatibility of the films was determined when the elongation at break of the films reached its peak. And the problem of insufficient elongation at break when chitosan/starch films were used as agricultural films was solved. The above studies showed that the mechanical properties of the chitosan/starch films had a great relationship with the hydrogen bond strength, crystallinity and the internal structure of the films. Therefore, in order to explain the different effects of plasticizing different components on the mechanical properties of the films, Fourier transform infrared (FTIR), spectroscopy and X-ray diffraction (XRD), and scanning electron microscopy (SEM) methods were used to characterize hydrogen bond strength, crystallinity, and internal structure of the films whose different components were plasticized.

2. Experimental

2.1. Experimental instruments and materials

Chitosan (95.0% deacetylation degree) with molecular weight of about 106 was purchased from Shandong Dongrun Biotechnology Co., Ltd. (Shandong, China). Corn starch of reagent grade and with an average particle diameter of 30 μm was purchased from Hebei Huachen Starch Sugar Co., Ltd. (Hebei, China). The general specifications are as follows: 12.5–13.0% moisture content, 0.20% ash, 0.20% pulp, pH value of 5–7. Glycerol (99.0% purity) and glycol (99.0% purity) as plasticizing agents were purchased from Tianjin Fuyu Fine Chemical Co., Ltd. (Tianjin, China). Urea of AR grade and with purity ≥99.0% was purchased from Tianjin Zhiyuan Chemical Reagent Co., Ltd. (Tianjin, China). Sodium hydroxide (NaOH) powder with purity ≥96.0% was purchased from Cangzhou Manyue Chemical Sales Co., Ltd. (Hebei, China).

HHS-2 electronic water bath with constant temperature was bought from Shanghai Kanglu Instrument Equipment Co., Ltd. JJ-1 precision booster was sourced from Cangzhou Boyuan Experimental Analytical Instrument Factory. Electronic balance (2000 g/0.01 g) was purchased from Shanghai Huachao Electric Co., Ltd. Electric thermostat blast drying oven was bought from Shanghai Jinghong Experimental Equipment Co., Ltd. The infrared spectrometer, BRUKER VERTEX-70, was obtained from Bruker, Germany. XLW (L)-PC intelligent electronic tension machine was sourced from Jinan Blu-ray Electromechanical Technology Co., Ltd. The scanning electron microscope (model FEG250) was purchased from Beijing Oubo Tong Optical Technology Co., Ltd. YS20B nickel–copper filter radiator was procured from Taizhou Yishun Valve Co., Ltd.

2.2. Film preparation

(1) To prepare the chitosan solution. We mixed and stirred 8 g of NaOH, 4 g of urea and 88 g of water to obtain the chitosan dissolution system with 8% NaOH and 4% urea.[29,30] Then, the chitosan powder was dispersed into the mixture, which was stirred for 20 min to obtain a chitosan suspension. Then we chilled this suspension to −30 °C and stirred it three times during this time. Finally, it was thawed at room temperature to obtain the transparent chitosan solution.

(2) To prepare the gelatinised starch. We poured 100 g of distilled water and 24 g of starch into beakers. The mixture was then stirred. A uniform suspension of the starch was obtained, and the beakers were placed in a water bath at a constant temperature of 80 °C. The contents were stirred using a blender for 30 min to obtain gelatinised starch.[31]

(3) To prepare films with different proportions of chitosan and starch. We mixed the chitosan solution and the gelatinised starch according to the ratio of starch : chitosan = 1 : 0, 1 : 0.5, 1 : 1, 1 : 1.5. And then we stirred them for 60 min with a magnetic stirrer to get the mixed slurry. Bubbles were removed through centrifugation. The mixed slurry was spread on a Teflon plastic sheet and was then placed in the dryer. The temperature of the dryer was kept at 80 °C. After drying for 3 h, the films were peeled off from the Teflon plastic mould. Then we carried out the mechanical test of the films according to the method of 2.2. The experimental results are shown in Fig. 1. The elongation at break (E) of the films increased first and then decreased as starch content increased. Thus, the ratio of chitosan to starch when the films had the highest E should be between 1 : 0–1 : 1.

Therefore, the concentration gradient was set to 0.2. We mixed the chitosan solution and the gelatinised starch according to the

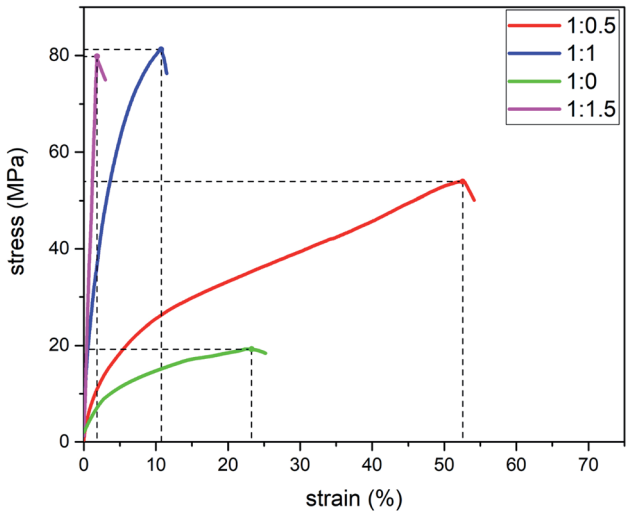

Fig. 1 Stress–strain (d–3) curves of different starch–chitosan films with various proportions in the pilot experiment.

ratio of starch : chitosan = 1 : 0.2, 1 : 0.4, 1 : 0.6, 1 : 0.8 and 1 : 1. Repeat the above process of preparing the films.

(4) To prepare the films with different plasticized ingredients. We used 7.5% glycerol to plasticize starch slurry (NS) and chitosan slurry (NC) to obtain plasticized starch (TPS) and plasticized chitosan (TPC). Then stand for 48 h. Using the optimal ratio obtained by testing in the (3), we prepared ordinary starch and ordinary chitosan (NS + NC), plasticized chitosan and ordinary starch (TPC + NS), plasticized starch and ordinary chitosan (TPS + NC) and plasticized chitosan and plasticized starch (TPS + TPC). Repeat the above process of preparing the films. The specific process is shown in Fig. 2.

(5) To prepare the films treated with different proportions of plasticizer. Using a uniform design experiment, we set glycerol and ethylene glycol as two factors, each of which was set with six levels with a concentration gradient of 2.5%. According to the uniform experimental table, we configured six different proportions of plasticizers as shown in Table 1. Based on the experimental results of (3) and (4), we plasticized the slurry using six plasticizers and allowed them to stand for 48 h. Repeat the above process of preparing the films.

Table 1 Different proportions of plasticizer

	1	2	3	4	5	6
Glycerine (g)	0	2.5	5	7.5	10	12.5
Glycol (g)	5	12.5	2.5	10	0	7.5

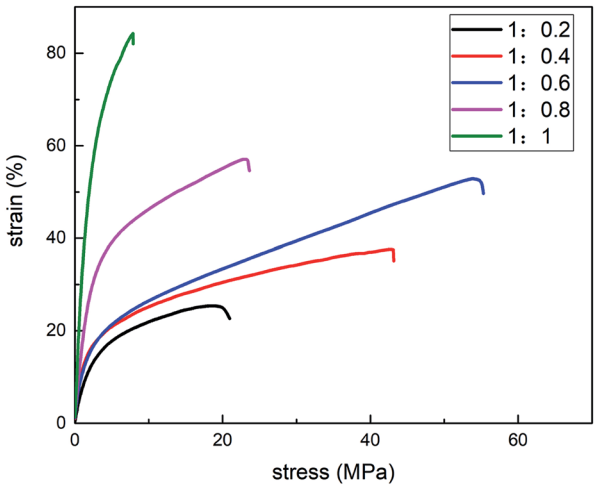

Fig. 3 Stress–strain (d–3) curves of different starch–chitosan films with various proportions.

2.3. Film tensile test

The obtained films were subjected to a standard pattern in accordance with the ASTM Standard Method D 882-91 (1995a). It was then subjected to a tensile test using an XLW (L)-PC type intelligent electronic tensile machine to measure the mechanical properties of tensile strength (TS) and elongation at break (E). The initial jig separation was set to 50 mm, and the cross-head speed was set to 100 mm min^{-1}. TS was expressed in MPa and was calculated by dividing the maximum load (N) by the initial cross-sectional area (m^2) of the sample. The E was calculated as the ratio of the final length of the sample break point to the initial length of the sample and was expressed as a percentage. Test each type of the films five times. The stress–strain curve of the sample was obtained by calculating and analysing the TS.

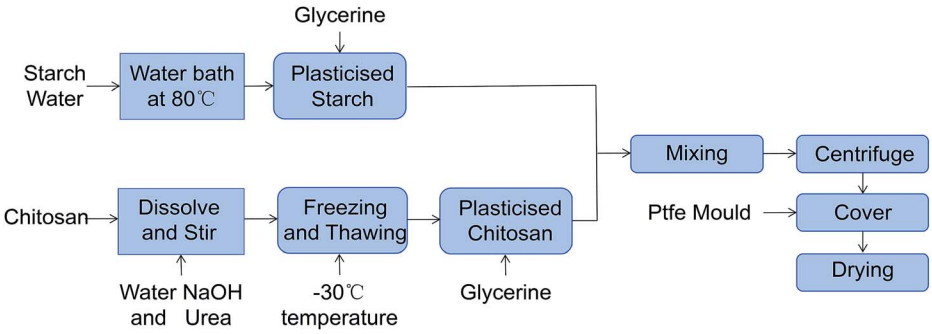

Fig. 2 Flow chart of composite films preparation.

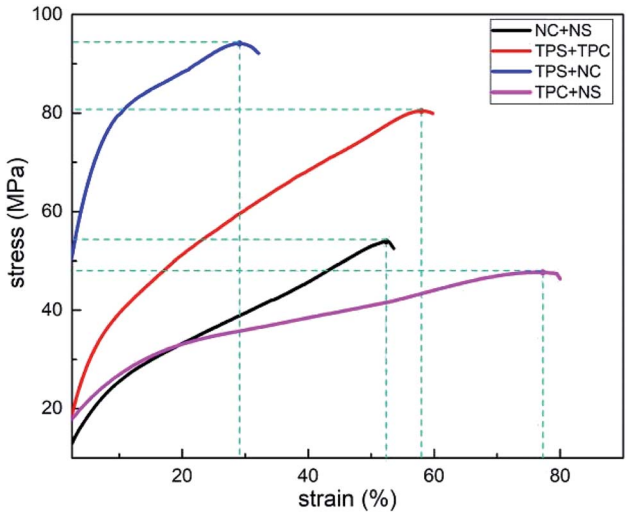

Fig. 4 Stress–strain (d–3) curves of NC + NS/TPC + TPS/TPS + NC/TPC + NS.

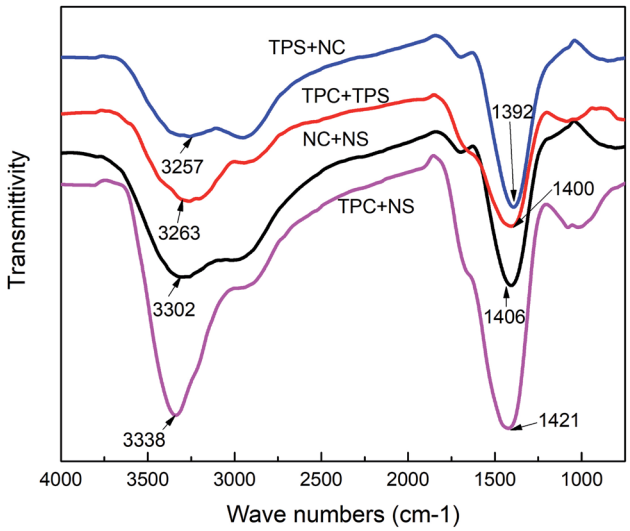

Fig. 5 Infrared spectra of NC + NS/TPC + TPS/TPS + NC/TPC + NS.

2.4. Microscopic testing of the film

(1) Infrared spectra analysis. Anhydrous NS + NC, TPS + NC, TPC + NS and TPS + TPC at approximately 5 mg each were mixed with 150 mg KBr and milled thoroughly to reach a particle diameter of <2.5 mm. The mixtures were compressed into pellets under approximately 10–12 MPa and analysed using a VERTEX-70 FTIR spectrometer. Spectra were recorded at a resolution of 2 cm^{-1} for 400–4000 cm^{-1}.

(2) X-ray diffraction experiments. The films were cut into the size of 10 × 10 mm^2. It was tested using a graphite curved crystal monochromator and nickel–copper filter radiator at room temperature. In the process of sample testing, the sample and glass frame should be flushed, and the sample should be smooth. The index of the seam system was DS/RS/SS = 1°/0.16 mm/1°. The test used Cu-Kα ray, Ni filter, tube pressure set to 35 KV, tube flow set to 25 mA, scan speed of 5 ° min^{-1} and analysis angle ($2q$) interval of 10–90°.

(3) Scanning electron microscopy on composites. The internal structure of the fracture surface of the NS + NC/TPC + NS/TPS + NC/TPC + TPS films were investigated using a scanning electron microscope (FEG250) with an accelerating voltage of 10 kV. Prior to the SEM observation, all samples were mounted on aluminium stubs with ribbons and sputter coated with gold to make them electrically conductive.

2.5. Optimised film performance test

We prepared the optimised film according to the results obtained in 2.2 and tested them for water vapor transmission rate and tensile test. The tensile test method is shown in 2.3. The water vapor transmission rate test method is as follows.

The water vapour transmission rate (g m^{-2} h^{-1}) was determined gravimetrically using the ASTM method E 96-95 (1995b).[23] The film sample was mounted on a polymethylmethacrylate cup containing 16 mL of distilled water. The cup was placed in an environmental chamber at 25 °C and relative humidity of 50%. The infiltrates were removed at a speed of about 200 m min^{-1} using a fan in the chamber. The weight of the beaker was recorded every 4 h for a total of 48 h. The water vapour transmission rate of the film in different time periods was calculated. Five films were taken for testing and averaging.

3. Results and discussion

3.1. Analysis of the effects of chitosan/starch ratio on the mechanical properties of films

The results are shown in Fig. 3. Given the chitosan–starch ratio ranging from 1 : 0.1 to 1 : 1, the TS gradually increased. In addition, the breaking elongation first increased and then decreased as starch content increased. The comparison

Table 2 Results of the data from the tensile tests/FTIR/XRD

Different plasticizing methods	NC + NS	TPC + NS	TPS + NC	TPC + TPS
Tensile strength (MPa)	53.9	47.7	93.4	80.4
Elongation at break (%)	52.6	76.3	29.1	58.3
FTIR peak frequency (cm^{-1})	3302	3338	3257	3263
	1406	1421	1392	1400
XRD 2θ (°)	29.14	29.10	20.96	21.04
	34.04	33.98	30.98	31.02

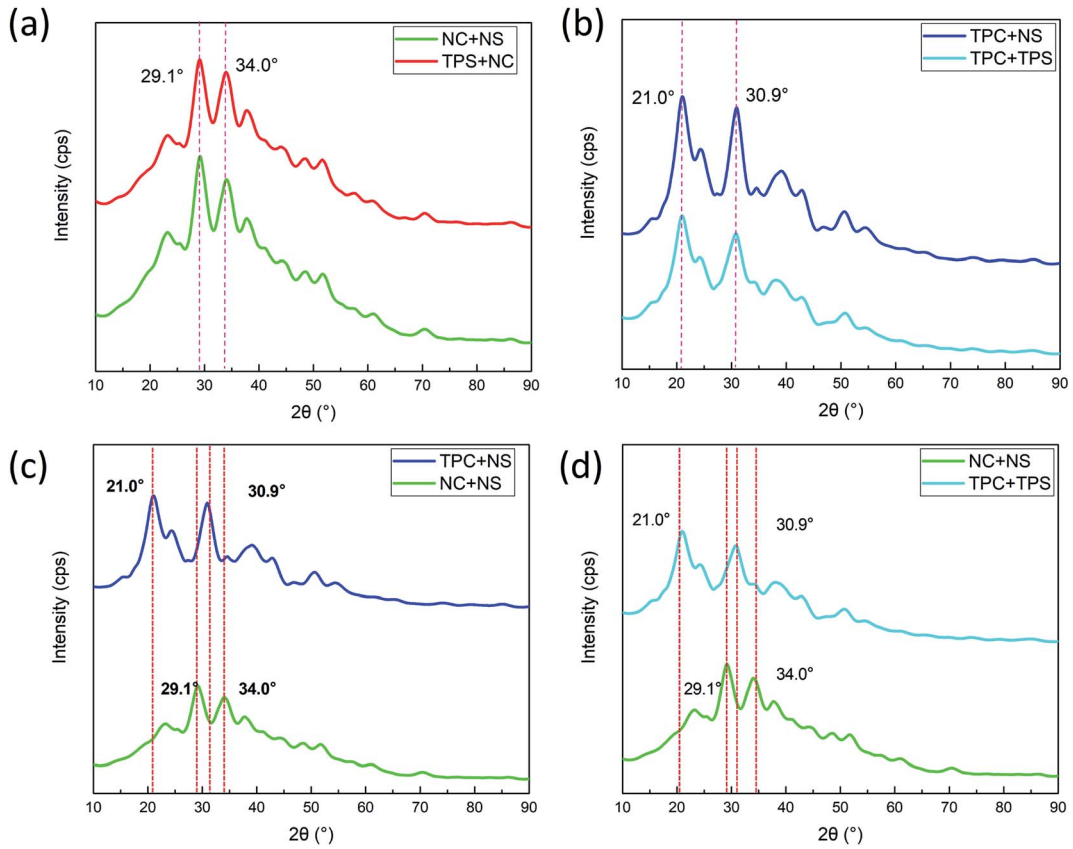

Fig. 6 X-ray diffraction curves of (a) NC + NS and TPS + NC; (b) TPC + NS and TPC + TPS; (c) NC + NS and TPC + NS; (d) NC + NS and TPC + TPS.

between the stress and strain curves showed that the elongation reached 53.9% when the chitosan–starch ratio was 1 : 0.6 and that the TS reached 52.9 MPa. Under this ratio, the films had the highest *E* and good TS.

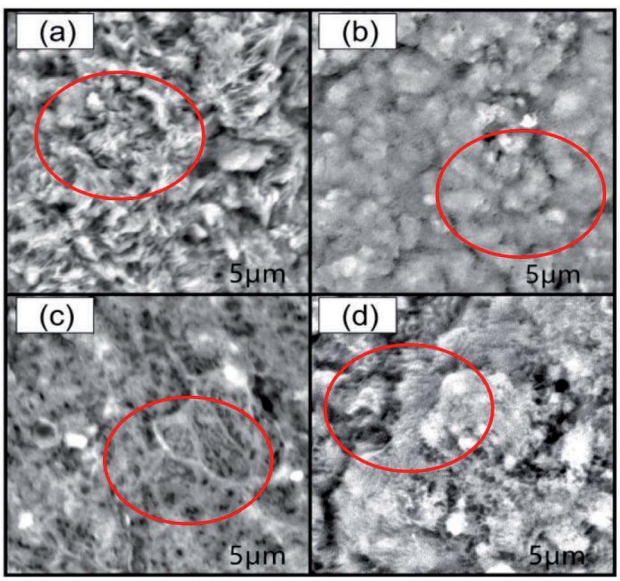

Fig. 7 SEM images of the internal structures of (a) NC + NS (b) TPS + NC (c) TPC + NS (d) TPC + TPS.

3.2. Effects of single/integral composition modification on mechanical properties of films

(1) Analysis of films tensile test. The tensile test results of a single/integrated plasticized films are shown in Fig. 4 and Table 2. Compared with that of NC + NC, the *E* of TPC + NS increased from 52.6% to 76.3%, marking an increase of 45%; however, the TS decreased by 6.2 MPa. The typical effects of addition of plasticizers to polysaccharide system on mechanical properties, such as an increase in elongation in break and decrease in tensile strength.[32,33] The TS of TPS + NC increased from 53.9 MPa to 93.39 MPa, but the *E* decreased by 55%. The TS and *E* of TPC + TPS improved, with the TS reaching 80.4 MPa and the *E* reaching 58.3%. The comparison showed that the plasticisation of the different components exerted various effects on the mechanical properties of the films. The *E* of the film was the greatest when only chitosan was plasticized. Therefore, the method of solely plasticizing chitosan was used to increase the *E* of the films. It was found that the maximum elongation at break reached 61.6%, and the tensile strength was close to 35 MPa in Xu's study.[23] Compared with the study of Xu, the elongation at break of the films in this study was much improved.

Table 3 *E* at different glycerol and glycol ratios

Glycerine (%)	0	2.5	5	7.5	10	12.5
Glycol (%)	5	12.5	2.5	10	0	7.5
Elongation at break (%)	57	70	12.9	72	78.6	43

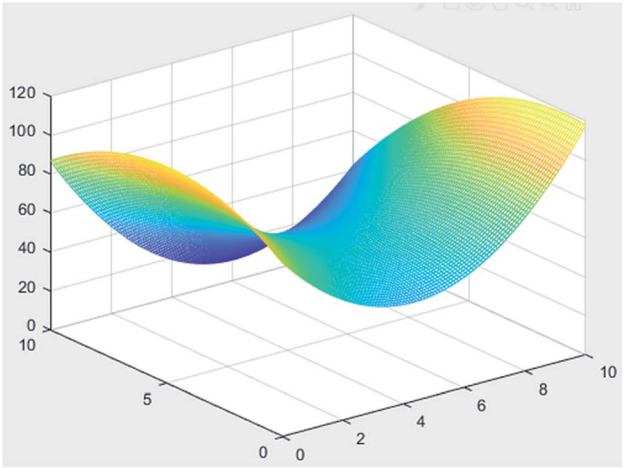

Fig. 8 3D contour plot of regression equation.

(2) **FTIR results.** The test results are shown in Fig. 5. The film spectrum is similar to previous reports.[23,24,28] In the FTIR spectrum, the absorption peak of OH stretching vibration is located at 3000–3600 cm^{-1}; the tensile absorption peak of NH is also in this interval. The two overlap.[23,34] The bending peak of NH is near 1500 cm^{-1}.[23] The overlapping absorption peaks of OH stretching and NH stretching of NC + NS were 3302 cm^{-1}, the NH bending absorption peak of NC + NS was 1392 cm^{-1}. Those of TPS + NC were 3257 and 1400 cm^{-1}. Those of TPC + NS were 3338 and 1406 cm^{-1}. Those of TPC + TPS were 3263 and 1421 cm^{-1}. When two or more substances are mixed, physical blends *versus* chemical interactions are reflected by changes in characteristic spectra peaks.[32] The formation of hydrogen bonds changed the vibrational frequency of the hydroxyl groups. Strong hydrogen bonds indicated a low vibrational frequency of the hydroxyl groups.[35] TPS + NC had the lowest absorption peak frequency and numerous OH and NH functional groups. They exposed the more hydrogen and oxygen atoms, which was conducive to the formation of hydrogen bonds between plasticizer, starch and chitosan. However, numerous hydrogen bonds hindered the sliding between molecular chains and made them less deformable.[18] Hence, the *E* was low. In contrast, TPC + NS had the highest absorption peak frequency. So its *E* was the highest. When only chitosan was plasticized, more OH of glycerol interacted strongly with chitosan–NH under the action of a low concentration of plasticizer.[24] This was shown in the peak moving from 3302 cm^{-1} (NC + NS) to 3338 cm^{-1} (TPC + NS). The TS of the film was reduced and the *E* was increased. Such hypothesis is well agreed with the concept of anti-plasticization effect caused by low-amount of plasticizer where the addition of plasticizers weakened strength of macromolecular interactions.[24,38]

(3) **XRD test results.** To verify the accuracy of the infrared spectrum, we performed XRD tests on the four films. The test results are shown in Fig. 6. Fig. 6(a)–(d) show the comparison of the XRD test results for NC + NS and TPS + NC; TPC + NS and TPC + TPS; NC + NS and TPC + NS; and NC + NS and TPC + TPS. NC + NS had the peaks at $2\theta = 29.14°$, 34.04°; TPS + NC had the peaks at $2\theta = 29.10°$, 33.98°. These peaks were similar, TPC + NS had the peaks at $2\theta = 20.96°$, 30.98°; TPC + TPS had the peaks at $2\theta = 21.04°$, 31.02°. These peaks were also similar. The peak of the crystallization peak is similar to the previous studies.[23,24] When processed and analysed using Jade software, the crystallinity index of NC + NS was significantly greater than that of TPS + NC. Previous studies have proved that relationship between tensile strength of composites and crystallinity index was evident. It also showed that as the crystallinity increased, the tensile strength decreased and the elongation at break increased.[36] The crystallisation zone of TPS + NC shrunk due to the modification, and the amorphous region was enlarged. Many branches were found in the amorphous zone. Such property was conducive to the combination of starch and chitosan and resulted in a large tensile force in the tensile test. The TS of the film was relatively high. The crystallinity index of TPC + TPS was also significantly lower than that of TPC + NS. Hence, the TS of TPC + TPS was significantly higher than that of TPC + NS. This phenomenon was consistent with the FTIR test results.

(4) **SEM test results.** To further understand the changes in the mechanical properties of the films from a microscopic point of view, we tested four films were tested using SEM. The results are shown in Fig. 7. Test results were similar to previous studies.[30] Fig. 7(a) presents the internal structure of NC + NS.

Table 4 Analysis of variance results (dependent variable: elongation at break)

Source	Class III square sum	Degree of freedom	Mean square	F	P
Modified model	46 496.704	12	3874.725	4278.468	0.000
Intercept	47 241.669	1	47 241.669	52 164.204	0.000
Ratio of chitosan to starch (*A*)	15 449.589	3	5149.863	5686.474	0.000
Plasticizing different components (*B*)	19 545.190	2	9772.595	10 790.890	0.000
Plasticizer ratio (*C*)	19 960.665	2	9980.332	11 020.273	0.000
$A \times B$	4017.218	1	4017.218	4435.809	0.000
$A \times C$	13.759	1	13.759	15.193	0.000
$B \times C$	1554.261	1	1554.261	1716.213	0.000
$A \times B \times C$	187.749	1	187.749	207.312	0.000
Error	47.093	52	0.906		
Total	143 121.185	65			
Total after correction	46 543.797	64			

The branched structure of chitosan was bound by starch to form a cluster structure. Fig. 7(b) shows the internal structure of TPS + NC. As shown in the figure, a block structure was formed. The blocks were tightly bonded and combined to form the film and thus increased the TS. However, producing deformation is difficult. Hence, the *E* decreased because the microstructure of the starch changed after the addition of glycerine and ethylene glycol. The compatibility or uniformity of the blended composite was improved.[37] The fine-grained starch granules could fill the various voids of the chitosan so that the mutual chitosan branches were tightly bonded and a massive structure was formed. Fig. 7(c) shows the internal structure of TPC + NS. A large-area network structure was formed and facilitated deformation during stretching. The *E* increased. The plasticizer connected the chitosan to form a network structure. The starch granules could only adhere to the surface of the chitosan because they were too large to fill the interstitial spaces. Fig. 7(d) shows the internal structure of TPC + TPS. TPC + TPS formed not only a sheet-like structure over a large area but also a network structure between the sheets. Hence, the sheet-like structures became combined. The starch granules filled the voids of the chitosan network structure, thereby forming a partly block structure. However, the gap between the plasticized chitosan network was large, resulting in the starch granules not completely filling. Therefore, a partial network structure remained. These phenomena are consistent with the results of the mechanical tests and prove the rationality of the XRD and FTIR results.

3.3. Analysis of the effects of plasticizer ratio on the mechanical properties of films

The results are shown in Table 3. The *E* of the film peaked at 78.6% when the glycerine concentration reached 10% and no ethylene glycol was applied. Further regression analysis of the films by MINTAB software showed that the regression equation model of *E* with glycerol and ethylene glycol is the formula (1).

$$Y = 89.29 - 17.78X_1 + 9.065X_2 + 20.64{X_1}^2 - 0.931{X_2}^2 - 0.7307X_1X_2 \quad (1)$$

Y represents the *E* of the films, X_1 represents the concentration of glycerol and X_2 represents the concentration of ethylene glycol.

MATLAB was used to analyse the regression equation, and the resulting 3D contour map is shown in Fig. 8. The concentration of glycerol and ethylene glycol was set in the range of 0–10%. (The study of M. J. Halimatul found that TS and *E* of the films would significantly decrease with the increase of

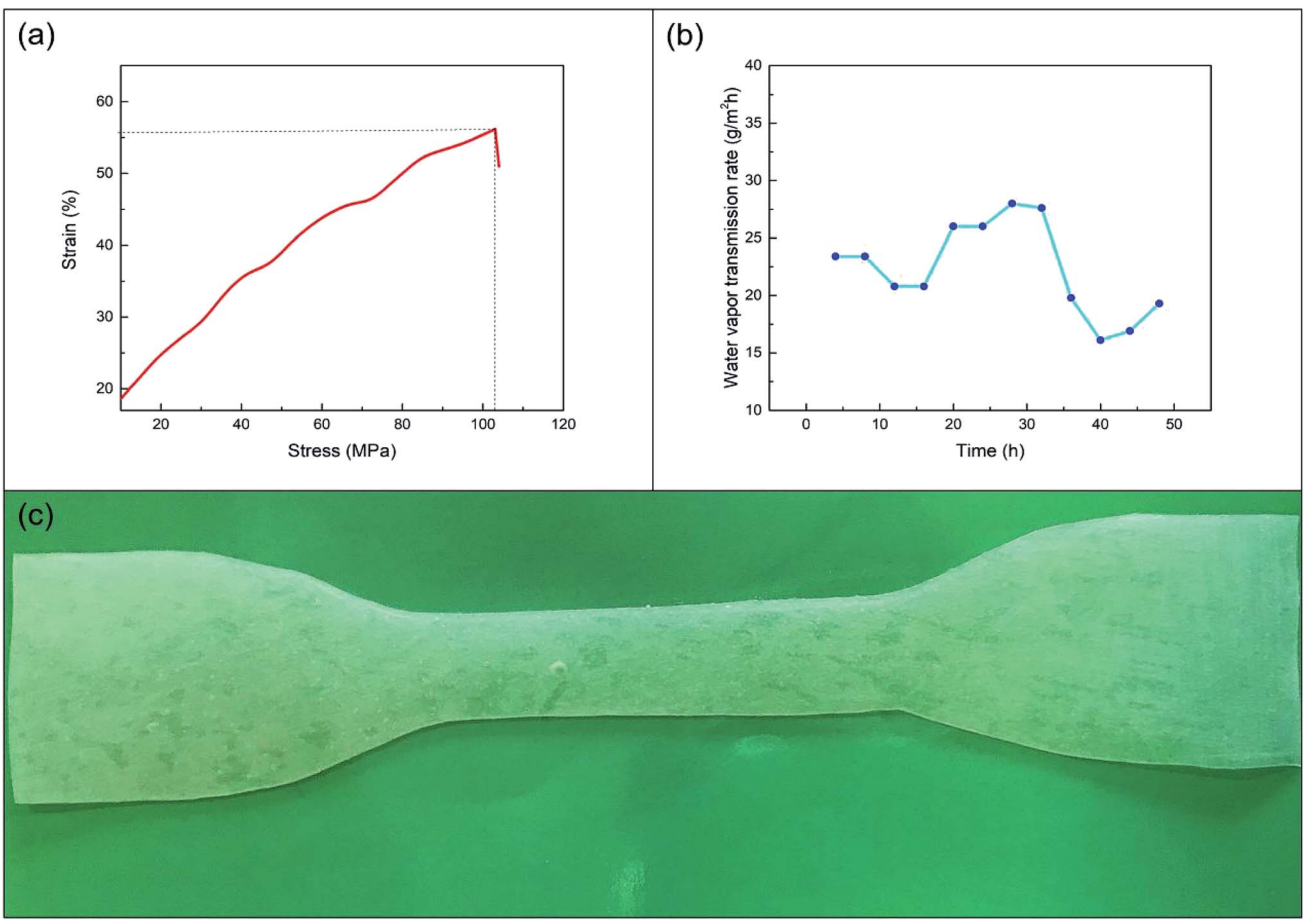

Fig. 9 Test results of (a) mechanical properties, (b) water vapour permeability and (c) film pictures.

plasticizer content when the plasticizer was above 10%.[39] So the concentration range was set within 10%.) The *E* of the film reached the maximum when the glycerol was 10 g and the ethylene glycol was 0.94 g. Model prediction results showed that the *E* of the film at this time reached 118.7%.

3.4. Analysis of variance test

Analysis of variance was conducted on all mechanical test data by SPSS software. The results of the analysis are shown in Table 4. The *P* values were all less than 0.05, the influence of different chitosan and starch ratios, different plasticizing components and different plasticizer ratios these three factors on the film *E* was very significant. And the interaction of the three factors mutual interaction of the three factors had a significant effect on the *E* of the films. Therefore, in this paper, it was reasonable to combine the three methods to improve the elongation at break of the film.

3.5. Performance testing

The tensile test result of the film is shown in Fig. 9(a). At this time, the *E* of the film reached 104.1%, and the TS was 56.18 MPa. Compared with previous studies, elongation at break was much improved.[23,24] Thus, the film had a high *E*. It also maintained a certain strength, and the mechanical properties of the film were satisfactory. The experimental test on the water vapour transmission rate of the film is presented in Fig. 9(b). The experimental results showed that the water vapour transmission rate was stable at about 20 g m^{-2} h^{-1}. The water vapour transmittance of the film was significantly lower than that of the films studied by Xu *et al.*[23] Fig. 9(c) shows that the light transmittance of the film was good. These performance results meet the requirements of agricultural films.

4. Conclusions

Among plasticizing films of different compositions, TPC + NS had the largest elongation at break and TPS + NC had the largest tensile strength. The results of XRD showed that mechanical properties of films were related to its crystallinity. The higher the crystallinity, the higher the elongation at break. Plasticizing starch alone facilitated the formation of hydrogen bonds and massive structure, supported by the results of FTIR and SEM respectively. Plasticizing chitosan alone was beneficial to the formation of network structure and exhibited anti-plasticization at low plasticizer concentration, supported by the results of SEM and FTIR respectively. The film prepared by mixing chitosan plasticized with 10% glycerol and 0.94% ethylene glycol alone to starch at a ratio of 1 : 0.6, had the highest elongation at break of up to 104.1%, with good tensile strength, water vapour barrier properties and light transmission. Such discovery can effectively solve the problem that chitosan/starch films often break, which is beneficial to its use as agricultural mulching films.

Conflicts of interest

There are no conflicts to declare.

Acknowledgements

This work was financially supported by National Natural Science Foundation of China (No. 51775318), National Natural Science Foundation of China (No. 51375278), and The Interdisciplinary Cultivation Project of Shandong University (No. 2018JC043). We would like to thank our colleagues from Shandong University.

References

1 J. R. Jambeck, R. Geyer, C. Wilcox, *et al.*, Plastic waste inputs from land into the ocean, *Science*, 2015, **347**(6223), 768–771.
2 W. D. Luzier, Materials Derived from Biomass/Biodegradable Materials, *Proc. Natl. Acad. Sci. U. S. A.*, 1992, **89**(3), 839–842.
3 T. W. Brooks, Apparatus for recycling previously used agricultural plastic film much, *J. Cleaner Prod.*, 1997, **5**(4), 318.
4 R. A. Ilyas, S. M. Sapuan, M. R. Ishak, *et al.*, Development and characterization of sugar palm nanocrystalline cellulose reinforced sugar palm starch bionanocomposites, *Carbohydr. Polym.*, 2018, **202**, 186–202.
5 F. H. Otey and R. P. Westhoff, Starch-based films. Preliminary diffusion evaluation, *Ind. Eng. Chem. Prod. Res. Dev.*, 2002, **23**(2), 284–287.
6 L. Ren, X. Yan, J. Zhou, *et al.*, Influence of chitosan concentration on mechanical and barrier properties of corn starch/chitosan films, *Int. J. Biol. Macromol.*, 2017, **105**(3), 1636–1643.
7 H. Abral, A. Basri, F. Muhammad, *et al.*, A simple method for improving the properties of the sago starch films prepared by using ultrasonication treatment, *Food Hydrocolloids*, 2019, **93**, 276–283.
8 S. Mali, L. S. Sakanaka, F. Yamashita, *et al.*, Water sorption and mechanical properties of cassava starch films and their relation to plasticizing effect, *Carbohydr. Polym.*, 2005, **60**(3), 283–289.
9 N. Laohakunjit and A. Noomhorm, Effect of Plasticizers on Mechanical and Barrier Properties of Rice Starch Film, *Starch*, 2004, **56**(8), 348–356.
10 Q. Chen, H. J. Yu, L. Wang, *et al.*, Recent progress in chemical modification of starch and its applications, *RSC Adv.*, 2015, **5**(83), 67459–67474.
11 N. Reddy and Y. Yang, Citric acid cross-linking of starch films, *Food Chem.*, 2015, **118**(3), 702–711.
12 R. A. Ilyas, S. M. Sapuan, M. R. Ishak, *et al.*, Isolation and characterization of nanocrystalline cellulose from sugar palm fibres (Arenga pinnata), *Carbohydr. Polym.*, 2017, **181**, 1038.
13 R. A. Ilyas, S. M. Sapuan, M. R. Ishak, *et al.*, Sugar palm (Arenga pinnata (Wurmb.) Merr) cellulosic fifibre hierarchy: a comprehensive approach from macro to nano scale, *J. Mater. Res. Technol.*, 2019, **8**(3), 2753–2766.

14 R. A. Ilyasa, S. M. Sapuan, M. R. Ishakc, *et al.*, Isolation and characterization of nanocrystalline cellulose from sugar palm fibres (Arenga pinnata), *Carbohydr. Polym.*, 2018, **181**, 1038–1051.

15 R. A. Ilyas, S. M. Sapuan, M. R. Ishak, *et al.*, Water Transport Properties of Bio-Nanocomposites Reinforced by Sugar Palm (Arenga pinnata) Nanofibrillated Cellulose, *Journal of Advanced Research in Fluid Mechanics and Thermal Sciences*, 2018, **51**(2), 234–246.

16 R. A. Ilyas, S. M. Sapuan, M. R. Ishak, *et al.*, Sugar palm nanocrystalline cellulose reinforced sugar palm starch composite: degradation and water-barrier properties, *IOP Conf. Ser.: Mater. Sci. Eng.*, 2018, **368**, 012006.

17 J. Bonilla, L. Atares, M. Vargas, *et al.*, Properties of wheat starch film-forming dispersions and films as affected by chitosan addition, *J. Food Eng.*, 2013, **114**(3), 303–312.

18 S. Mathew, M. Brahmakumar and T. E. Abraham, Microstructural imaging and characterization of the mechanical, chemical, thermal, and swelling properties of starch-chitosan blend films, *Biopolymers*, 2006, **82**, 176–187.

19 J. Bonilla, L. Atares, M. Vargas and A. Chiralt, Properties of wheat starch film-forming dispersions and films as affected by chitosan addition, *Food Eng.*, 2013, **114**, 303–312.

20 M. Kong, X. G. Chen, K. Xing, *et al.*, Antimicrobial properties of chitosan and mode of action: a state of the art review, *Int. J. Food Microbiol.*, 2010, **144**(1), 51–63.

21 S. I. Park, M. A. Daeschel and Y. Zhao, Functional properties of antimicrobial lysozyme–chitosan composite films, *J. Food Sci.*, 2004, **69**(8), M215–M221.

22 C. Xiao, L. Zhu, W. Luo, X. Song and Y. Deng, Combined action of pure oxygen pretreatment and chitosan coating incorporated with rosemary extracts on the quality of fresh-cut pears, *Food Chem.*, 2010, **121**(4), 1003–1009.

23 X. Y. Xu, K. M. Kim, M. A. Hanna, *et al.*, Chitosan–starch composite film: preparation and characterization, *Ind. Crops Prod.*, 2005, **21**(2), 185–192.

24 H. H. Liu, R. Adhikari, Q. P. Guo and B. Adhikari, Preparation and characterization of glycerol plasticized (high-amylose) starch-chitosan films, *Food Eng.*, 2013, **116**, 588–597.

25 C. Bangyekan, D. Aht-Ong and K. Srikulkit, Preparation and properties evaluation of chitosan-coated cassava starch films, *Carbohydr. Polym.*, 2006, **63**(1), 61–71.

26 D. Attila, B. Janos and P. Klara, Understanding of the Plasticizing Effects of Glycerol and PEG 400 on Chitosan Films Using Solid-State NMR Spectroscopy, *Macromolecules*, 2009, **42**(13), 4667–4673.

27 M. F. Cervera, M. Karjalainen, S. Airaksinen, *et al.*, Physical stability and moisture sorption of aqueous chitosan–amylose starch films plasticized with polyols, *Eur. J. Pharm. Biopharm.*, 2004, **58**(1), 76.

28 M. O. Tuhin, N. Rahman, M. E. Haque, *et al.*, Modification of mechanical and thermal property of chitosan–starch blend films, *Radiat. Phys. Chem.*, 2012, **81**(10), 1659–1668.

29 X. Hu, Y. Du, Y. Tang, *et al.*, Solubility and property of chitin in NaOH/urea aqueous solution, *Carbohydr. Polym.*, 2007, **70**(4), 451–458.

30 B. Duan, B. Y. Liu, L. N. Zhang, *et al.*, Intermolecular interaction and the extended wormlike chain conformation of chitin in NaOH/urea aqueous solution, *Biomacromolecules*, 2015, 1410–1417.

31 C. W. Zhang, F. Y. Li, J. F. Li, *et al.*, A new biodegradable composite with open cell by combining modified starch and plant fibers, *Mater. Des.*, 2017, **120**, 222–229.

32 Y. Guan, X. Liu, Y. Zhang, *et al.*, Study of phase behavior on chitosan/viscose rayon blend film, *J. Appl. Polym. Sci.*, 1998, **67**(12), 1965–1972.

33 G. C. Ritthidej, T. Phaechamud and T. Koizumi, Moist heat treatment on physicochemical change of chitosan salt films, *Int. J. Pharm.*, 2002, **232**(1), 11–22.

34 M. A. Garcia, A. Pinotti and N. E. Zaritzky, Physicochemical, Water Vapor Barrier and Mechanical Properties of Corn Starch and Chitosan Composite Films, *Starch/Staerke*, 2006, **58**(9), 453–463.

35 S. W. Kuo, C. F. Huang and F. C. Chang, Study of hydrogen-bonding strength in poly(epsilon–caprolactone) blends by DSC and FTIR, *J. Polym. Sci., Part B: Polym. Phys.*, 2001, **39**(12), 1348–1359.

36 C. W. Zhang, F. Y. Li, J. F. Li, *et al.*, Novel treatments for compatibility of plant fiber and starch by forming new hydrogen bonds, *J. Cleaner Prod.*, 2018, **185**, 357–365.

37 X. S. Wu, Effect of Glycerin and Starch Crosslinking on Molecular Compatibility of Biodegradable Poly (lactic acid)-Starch Composites, *J. Polym. Environ.*, 2011, **19**(4), 912–917.

38 R. A. Talja, H. Helen, Y. H. Roos, *et al.*, Effect of various polyols and polyol contents on physical and mechanical properties of potato starch-based films, *Carbohydr. Polym.*, 2007, **67**(3), 288–295.

39 M. J. Halimatul, S. M. Sapuan, M. Jawaid, *et al.*, Effect of sago starch and plasticizer content on the properties of thermoplastic films: mechanical testing and cyclic soaking-drying, *Polimery*, 2019, **64**, 32–41.